

Optimality Criteria Solution Strategies in Multiple-Constraint Design Optimization

R. Levy*

Jet Propulsion Laboratory, California Institute of Technology, Pasadena, Calif.

and

W. Parzynski†

Montclair State College, Montclair, N. J.

Procedures and solution strategies to solve the conventional structural optimization problem using the Lagrange multiplier technique are described. The multipliers, obtained through solution of an auxiliary nonlinear optimization problem, lead to optimality criteria to determine the design variables. It is shown that this procedure is essentially equivalent to an alternative formulation using a dual-method Lagrangian function objective. Although mathematical formulations are straightforward, successful applications and computational efficiency depend upon execution procedure strategies. Strategies examined, with application examples, include selection of active constraints, move limits, and side constraint boundaries.

Introduction

THE structural design optimization problem has had significant attention at the research level during the past decade. Alternative mathematical formulations have been developed, and a number of diverse algorithms and solution strategies have been applied and tested on problems. The test problems, although usually representing structural models with only small numbers of displacement degrees of freedom and design variables, illustrate particular features that could be encountered when applied to the design of larger structures. As a result, current solution approaches have matured sufficiently for application to the practical design of large, complex structures.

The design problem is to minimize an objective function of the design variables, subject to primary inequality constraints. These constraints establish maximum permissible displacements and member stresses. An additional auxiliary set of side constraints limits the regions of acceptable design variables. The objective function considered here is the total weight of the structure; the design variables are rod cross-sectional areas or plate thicknesses.

Existing mathematical formulations have evolved within two categories: direct¹ and indirect.² Nonlinear programming methods are used in the first category to solve for all the design variables directly. For the second category, the problem is subdivided into two phases: first, the development of optimality criteria; and second, the application of these criteria to determine the design variables. The size of the solution space for the direct approach is equal to the number of design variables, whereas the solution space for the indirect approach is frequently of a much smaller size. As the result of smaller computation requirements for larger problem-size capability, the indirect methods currently appear to be favored.

An indirect approach is described here in which the Kuhn-Tucker conditions are used to formulate the problem. This permits the design variables to be computed readily from a small set of Lagrange multipliers by simple optimality criteria dependence relations. Since there is exactly one multiplier to

be determined for each primary constraint, the size of this set of multipliers is equal to the number of constraints that are active at the solution. The number of active constraints is typically much less than the total number of primary constraints. Hence, a few Lagrange multipliers determine many design variables by optimality criteria.

The essential part of the procedure, therefore, is to find the Lagrange multipliers by solving simultaneous nonlinear equations that are formulated in terms of the active constraint equations. An iterative method, such as Newton's method, or a modification thereof, is used to solve the system. This same system of equations arises in a formulation of the problem by Schmit and Fleury³ wherein a dual Lagrangian function is established as the objective and multipliers are chosen to maximize this function. This formulation appears to have produced the most effective results to date for a number of test problems. Both formulations are mathematically equivalent. The optimality criteria are the same; although in solving for the multipliers by Newton's method, the coefficient matrix in one case is the Jacobian of the constraints and in the other it is the Hessian of the dual function, these matrices are identical.

Although the foregoing procedures are conceptually well established, successful application and execution efficiency can depend upon the effectiveness of several strategies employed during implementation. The primary concern here is to describe alternative strategies and discuss their effectiveness.

Problem Identification

The class of structures includes those for which the displacement degrees of freedom at the nodes of the analytical model consist of the three translations in an *X-Y-Z* Cartesian coordinate system. Consequently, the finite elements in these structures are either one-dimensional rod elements or membrane-type plates, for which the design variables are the rod cross-sectional areas or the plate thicknesses. Although beam elements are excluded, the applications include many types of practical structures, such as trusses, transmission towers, aircraft components, and radar antennas. As a simplification, it is assumed here that all structural members are of the same material; consequently, the objective of minimizing total structure volume is equivalent to minimizing structure weight.

Primary displacement constraints are developed by a virtual work formulation in which displacement of the

Presented as Paper 81-0551 at the AIAA/ASME/ASCE/AHS 22nd Structures, Structural Dynamics and Materials Conference, Atlanta, Ga., April 6-8, 1981; submitted April 13, 1981; revision received Oct. 5, 1981. Released to AIAA to publish in all forms.

*Member of the Technical Staff. Member AIAA.

†Associate Professor of Mathematics and Computer Science.

structure is represented as the summation of the virtual work for individual members when a unit virtual load is applied to the structure at the node and in the direction of the constrained displacement. Stress constraints are converted to displacement constraints, and the corresponding virtual load for bar stresses consists of a pair of unit loads directed along the axis of the bar. Virtual loads for plate elements can also be developed by a similar, although more complex, procedure.⁴

Since each primary stress constraint requires a virtual loading vector and a corresponding load-displacement analysis, substantial computation time can be required to process large numbers of stress constraints. In the case of large-structure models, in addition to the computation time for numerical processing of virtual loading vectors, significant time could be required to reread the stiffness matrix decomposition back into core as needed to compute virtual displacements.⁵ Stress ratio constraints are a much simpler, although frequently unreliable, alternative to developing primary stress constraints for particular members. Stress ratio constraints establish minimum design variables that are equal to the current value times the ratio of current stress to allowable stress.

In addition to requirements for the primary constraints are restrictions that the side constraints impose on selection of design variables. A number of individual structural members can be assembled into groups with common design properties. Upper or lower bounds upon the admissible selection of design variables, stress ratio constraints, and move limits can be prescribed. Since the design process is iterative and extends through a number of design cycles, move limits can restrict the cyclic changes in the design variables.

Mathematical Formulation

A large class of structural optimization problems can be formulated in terms of the following nonlinear mathematical programming problem:

Minimize

$$V = \sum_{i=1}^N L_i a_i \quad (1)$$

subject to the constraints

$$G_j = \sum_{i=1}^N \frac{F_{ij} L_i}{a_i} - C_j^* \leq 0 \quad j = 1, \dots, K \quad (2)$$

and

$$a_i \leq a_i \leq \bar{a}_i \quad i = 1, \dots, N \quad (3)$$

where the design variables a_i are the group cross-sectional areas of the member rods or plate thicknesses, L_i are the group lengths of the rods or plate planar areas, and F_{ij} is an internal stress resultant coefficient such that the virtual work of the i th structural design variable group for the j th constraint is $F_{ij} L_i / a_i$. The combined term $F_{ij} L_i$ is referred to as the "flexibility coefficient."⁴ The C_j^* is a bound on the virtual work, and \underline{a}_i and \bar{a}_i are lower and upper side constraint bounds, respectively, on the design variable a_i .

The Kuhn-Tucker conditions for this problem are given by⁶

$$\nabla V + \sum_{j=1}^K \lambda_j \nabla G_j = 0 \quad (4)$$

$$\sum_{j=1}^K \lambda_j G_j = 0 \quad (5)$$

$$\lambda_j \geq 0 \quad j = 1, \dots, K \quad (6)$$

where $\nabla(\cdot)$ indicates the gradient vector and λ_j are the Lagrange multipliers. Equation (4) yields the optimality criteria

$$a_i^2 = \sum_{j=1}^K F_{ij} \lambda_j \quad i = 1, \dots, N \quad (7)$$

and Eq. (5) together with the inequalities (2) and (6) imply

$$\lambda_j G_j = 0 \quad j = 1, \dots, K \quad (8)$$

thus requiring that for each j either $\lambda_j = 0$ or $G_j = 0$. In each stage of the iterative process a set of indices Q is identified as the active constraint set, we seek a solution of the simultaneous equations:

$$G_j = 0 \quad j \in Q \quad (9)$$

and all other λ_j are set equal to zero.

This is equivalent to the formulation by Schmit and Fleury,³ which introduces a dual function. Maximize

$$\ell(\lambda) = \sum_{i=1}^N L_i a_i + \sum_{j \in Q} \lambda_j G_j \quad (10)$$

subject to the optimality criteria (7), and

$$\lambda_j \geq 0 \quad j \in Q \quad (11)$$

If, in using Eq. (7), $a_i < \underline{a}_i$, then a_i is changed to \underline{a}_i ; if $a_i > \bar{a}_i$, then a_i is changed to \bar{a}_i . When the gradient of the dual function is set equal to zero, the system of Eqs. (9) results. Hence both formulations are equivalent and differences occur only in the methods and strategies of solution.

To solve the set of simultaneous Eqs. (9) subject to the optimality criteria (7), we use an iterative method that updates the n th iteration by

$$\lambda(n+1) = \lambda(n) - tS \quad (12)$$

where λ is a column vector of λ_j , t a search parameter, and S the search direction vector given by

$$S = [J]^{-1} G \quad (13)$$

in which G_j is a column vector with components G_j , and $[J]$ is the Jacobian matrix with entries

$$J_{kj} = \frac{\partial G_k}{\partial \lambda_j} \quad k, j \in Q$$

Equations (12) and (13) constitute a modified Newton method. When t is unity, it provides a normal Newton step, and then Eq. (12) represents the usual Newton method. By using the optimality criteria, the terms of the Jacobian are obtained:

$$\frac{\partial G_k}{\partial \lambda_j} = \sum_{i=1}^N \frac{\partial G_k}{\partial a_i} \frac{\partial a_i}{\partial \lambda_j} = -\frac{1}{2} \sum_{i=1}^N \frac{F_{ik} L_i F_{ij}}{a_i^3} \quad (14)$$

If any of the a_i , say a_p , has been set to one of the side constraint bounds, then the change in a_p is zero and the p th term in Eq. (14) should be omitted. The design variables of the a_p type are temporarily passive and the remainder active.

A feasibility upper bound on the positive parameter t is obtained from the restriction that $\lambda_j \geq 0$. If any of the components of S is positive, this bound becomes

$$d = \min_{s_j > 0} (\lambda_n / S_j) \quad (15)$$

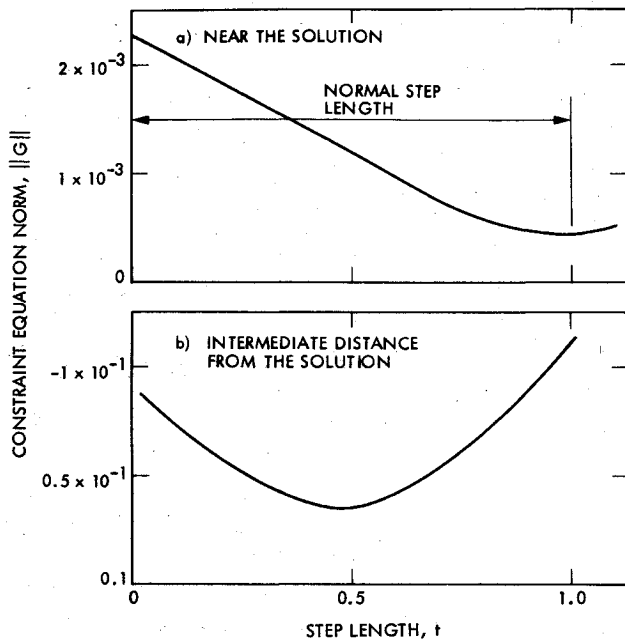


Fig. 1 Line search curves.

Then a line search is done on the smaller of the intervals $[0,1]$ and $[0,d]$ to find a value for t such that the norm of G

$$\|G\| = \sqrt{\sum_{j \in Q} G_j^2} \quad (16)$$

is a minimum. If $\|G\|$ is less than some acceptance tolerance ϵ , then convergence has been achieved and the next cycle is begun. If $\|G\|$ is not sufficiently small, then another iteration is performed in the new direction that is determined at the last point where Eq. (16) was evaluated.

Examining the behavior of $F(t) = \|G\|$ at $t=0$, the slope $F'(0) = -\|G\|$. Thus a small step in the Newton direction will decrease $F(t)$. However, over the interval $[0,1]$ several different types of behavior of $F(t)$ can occur. If λ is relatively close to the solution, $F(t)$ is almost linear to zero (see Fig. 1a). In some cases for λ not close to the solution, the graph of $F(t)$ has a minimum between $t=0$ and $t=1$ (see Fig. 1b). Since a variety of curve shapes can occur, a line search for the minimum can be useful.

Solution Strategies

A number of strategies are entailed in the details of applying the foregoing mathematics to obtain efficient numerical solutions and useful designs. Those to be discussed here include identification of the active constraint set, estimation of initial values for multipliers in the set, treatment of side constraints, and move limits.

An in-house research computer program incorporates these strategies. This is a small-problem program developed to explore the effects of strategies, algorithms, and parameter options before incorporation within the much-larger-capacity JPL-IDEAS program.⁷

Active-Constraint Set

A traditional difficulty associated with the use of Lagrange multipliers is to define the index set Q of active constraints (and nonzero multipliers) required to proceed with the solution of Eq. (9). Some approaches let Q represent all the K -constraint equations and add K additional slack variables.⁸⁻¹⁰ Other methods include all of the constraint equations at the outset and subsequently eliminate passive constraints identified by multipliers that approach zero.²

Another approach, which has produced the best results to date with our research program, has been more recently proposed by Fleury and Schmit.³ They recommend building up the set of active constraints one constraint at a time in order of increasing severity.

The severity of the constraint equations can be examined in terms of the numerical order of constraint ratios D_j , expressed as

$$D_j = C_j / C_j^* \quad (17)$$

where C_j is the first term of the right-hand side of Eq. (2), i.e.,

$$C_j = \sum_{i=1}^N \frac{F_{ij} L_i}{a_i} \quad (18)$$

Our procedure at the start of each design cycle is to identify the largest ratio and then compute the associated multiplier λ_j directly from an equation applicable in the case of a single constraint requirement. The equation is

$$\lambda_j^{1/2} = \sum_{i=1}^N \frac{(F_{ij})^{1/2} L_i}{C_j^* - C_j^p} \quad (19)$$

in which the numerator excludes contributions from passive design variables and C_j^p in the denominator is the virtual work of the passive variables. This equation is applied sequentially until the set of active and passive design variables stabilizes. At first all design variables are taken to be active unless specifically excluded from redesign by the program user or unless F_{ij} is negative. The first trial value found for λ_j is used to compute the values of the active set of design variables according to the decoupled form of Eq. (7):

$$a_i^2 = F_{ij} \lambda_j \quad (20)$$

These are examined for side constraint boundary violations [as described in the use of Eq. (7)], and the set of passive variables is appended accordingly. Then Eq. (19) is recomputed using the remaining active design variables. After a few repetitions of this process, the composition of the active and passive set usually becomes fixed. There will be eventual convergence of λ_j unless all design variables have been transferred to the passive set. If all variables become bounded, alternative remedial measures can be considered.

Once λ_j has been obtained, the constraint equations are recomputed using the corresponding optimality criteria computations for the design variables. If there are no constraint violations, the current design cycle is completed, and reanalysis of the structure with the new set of design variables initiates the next cycle.

More frequently, however, there will be constraint violations. Then the violated constraint with the largest constraint ratio is added to the active set, and Newton's method [Eqs. (12-16)] is used to compute the multipliers that satisfy the current set of active constraints. If there are violations of constraints not in the active set, the worst of these is added and Newton's method is applied again. Conversely, a constraint with multiplier approaching zero in the Newton method solution is removed from the active set. When no new constraints become active when computed with the current set of design variables, the design cycle terminates.

As constraints are added, two approaches for estimating the initial values for the next associated multiplier λ_n can be applied:

1) Use the value existing from a prior design cycle. If the particular constraint was not active previously, this implies zero as the estimate.

2) Use the approximation

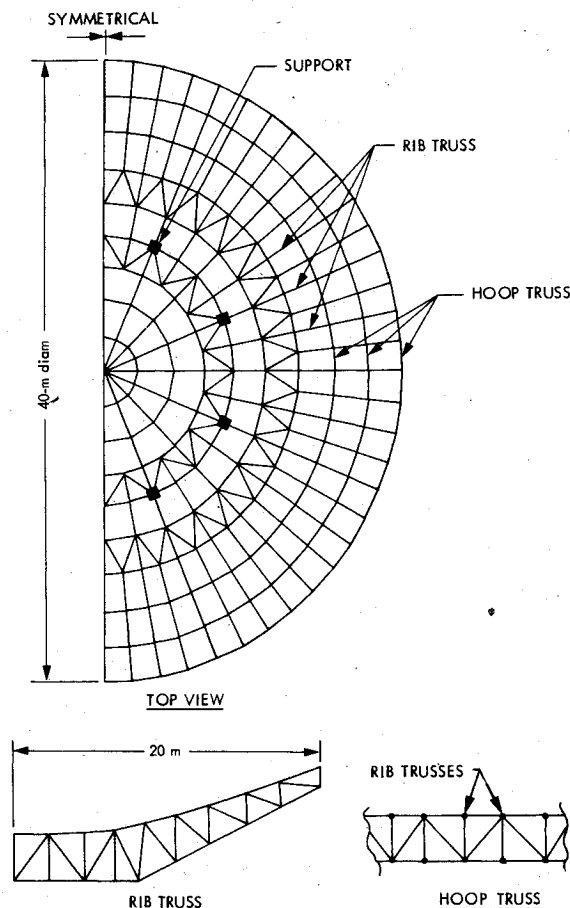


Fig. 2 Antenna backup structure.

$$\lambda_n \approx (V/C_n^*) (A_n - I); \quad A_n = \min(2, D_n) \quad (21)$$

in which the first ratio on the right is a decoupled estimate that ignores side constraints and can be derived from Eqs. (19) and (20). The second term in parentheses is a correction factor used to reduce the decoupled estimate of λ_n when the n th constraint equation is almost satisfied by the multipliers for the remaining active-constraint equations.

Because designs tend to stabilize after the early cycles and multipliers tend to become more consistent, our current practice is to use approach 2 for the first few cycles and approach 1 for the later cycles.

Move Limits

In this and almost all other mathematical formulations of the design problem is the assumption that during each design cycle the current distribution of internal stress resultants will not change significantly in the next cycle. Consequently, although the current design is reanalyzed at the beginning of each cycle and the stress resultant (internal force) distribution recomputed, changes in the F_{ij} terms that can take place in the next cycle are ignored. Although these changes do not occur in a statically determinate structure, they can become significant as the order of redundancy of the structure increases.

Move limits restrict the permissible design variable changes between adjacent cycles and are used to prevent significant internal force redistribution and thereby improve the accuracy of the design when projected to the next cycle. A move limit ratio R can set side constraint bounds for the design variable according to

$$\underline{a}_i = a_i / R \quad \bar{a}_i = a_i R \quad (22)$$

where the lower and upper bounds \underline{a}_i and \bar{a}_i are used in Eq. (3) and a_i is the value at the beginning of the cycle. If, however,

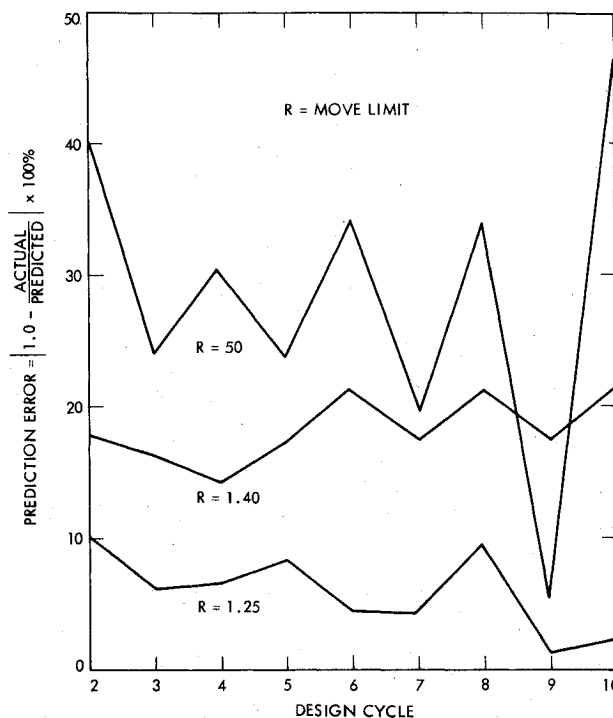


Fig. 3 Virtual work prediction error, 40-m (132-ft) reflector.

there are also stress ratio bounds or initial minimum or maximum size specifications, the boundary sizes given by Eqs. (22) may have to be readjusted to the most restrictive of all these bounds.

One way to examine the extent of redundancy and the need for move limits is through the accuracy of predicting the virtual work associated with each constraint from one cycle to the next. When a new set of design variables is determined at the end of one cycle, Eq. (18) gives the predicted virtual work for the j th constraint. Recomputation of the virtual work at the beginning of the next cycle with the new set of F_{ij} terms provides the actual virtual work. The differences of ratios of predicted to actual virtual work from unity can be taken as the prediction error.

To illustrate the influence of various move limits upon prediction error, they were varied within several trial designs performed for the backup structure of a 40-m- (132-ft-) diam antenna/reflector structure. The backup structure format comprises radial rib trusses with interconnecting circumferential hoop trusses. Figure 2 shows the top view of the structural arrangement and side views of typical rib and hoop trusses. The analytical model contains 340 nodes and 1150 bar members and has a redundancy of about 180 degrees of freedom. There are 67 design variable groups that represent all the bar layout fabrication variations. The design was for wind loadings on the structure, with primary compliance constraints on the rms microwave pathlength error deviations from the best-fitting paraboloid.¹¹ Equal constraints were specified for three different orientations of the structure relative to the direction of the wind.

The first wind loading case treated was typically the severest and produced the largest constraint ratios. Figure 3 shows the prediction errors associated with the first constraint case for the move limits of $R = 1.25$, 1.40 , and 5.0 for 10 design cycles. The lowest move limit provides the smallest error; the errors of the larger move limits appear to be substantial. Data were also developed for $R = 10.0$, but the prediction errors were so large that they could not be plotted to the scale of the figure. Continuing the designs for additional cycles showed that the prediction errors for $R = 1.25$ stabilized to less than 4% but that there was no stabilization of the large excursions shown during the first 10 cycles for $R = 5.0$ or larger.

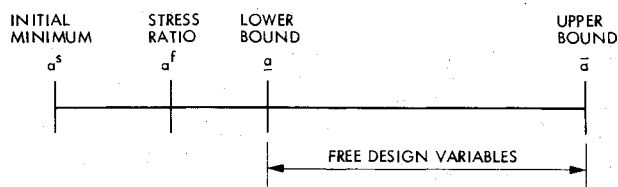


Fig. 4 Side constraint boundaries.

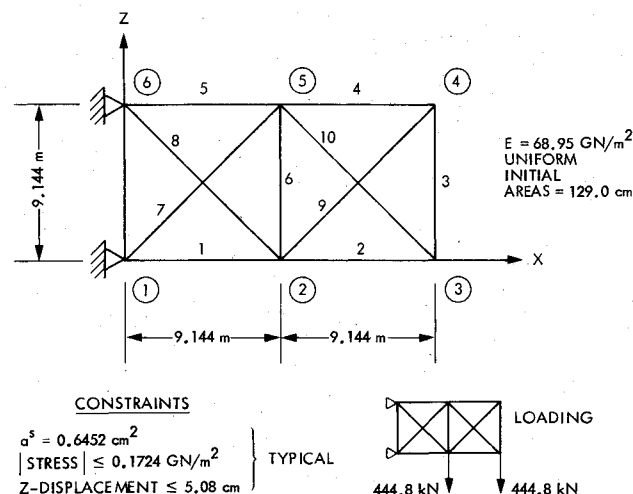


Fig. 5 10-bar truss.

Side Bounds

The move limits, preestablished minimum sizes, and stress ratio bounds are used to establish the side constraint boundaries at each design cycle for each design variable. The relevant terms for the i th design variable are, in ascending magnitude:

a_i^s = prespecified minimum size

a_i^f = minimum size required by stress ratio (if applicable)

a_i = minimum size allowed by move limit [Eq. (22)]

\bar{a}_i = maximum size allowed by move limit [Eq. (22)]

These terms are adjusted as necessary for consistency so that the stress ratio bound does not cancel the prespecified minimum and the lower move limit bound does not cancel the stress ratio bound. That is,

$$a_i^f = \max(a_i^f, a_i^s) \quad (23a)$$

and

$$\bar{a}_i = \max(\bar{a}_i, a_i^f) \quad (23b)$$

When a primary constraint replaces a stress ratio bound, Eq. (23a) is not used and Eq. (23b) becomes

$$\bar{a}_i = \max(\bar{a}_i, a_i^s) \quad (23c)$$

Then, from Eqs. (23), a design variable does not violate side constraints and can be evaluated according to the optimality criteria [Eq. (7)] when it satisfies the condition

$$a_i \leq a_i \leq \bar{a}_i \quad (24)$$

in which the limits above are recomputed at each design cycle. Figure 4 shows the relative position of these side constraints.

The move limit effect, when incorporated in the side constraint requirements, can be pivotal in the design procedure. As illustrated here by the backup structure example and elsewhere,² large move limits can be a source of error and small move limits can result in slow design progress. Unfortunately, the a priori specification of move limits is difficult since appropriate choices seem to be problem-dependent.

A converse to the requirement of stabilizing the design procedure by adopting small move limits is provided by the well-known 10-bar truss example problem, which shows that rapid convergence is hampered as the move limit is reduced. The configuration, specifications, and loadings are provided in Fig. 5. Table 1 shows the design histories with three move limit variations: $R \geq 50$, $R = 1.75$, and $R = 1.40$. These three designs were obtained with the ACCESS 3 program.³

The design cycles indicated are those that began with the corresponding tabulated weights. Consequently, the number of optimization cycles is always one less than the cycle shown. The tables end at the cycle that achieved the lowest feasible weight.

Table 1 shows the fewest number of design cycles required for the largest move limit (which is effectively no move limit

Table 1 ACCESS 3 program histories for 10-bar truss

Cycle	Structure weight scaled to feasible, kg (lbm)					
	$R = 1.0 \times 10^{30}$		$R = 1.75$		$R = 1.40$	
1	3749.5	(8266.2)	3749.5	(8266.2)	3749.5	(8266.2)
2	2718.6	(5993.5)	3436.5	(7576.2)	3794.5	(8365.5)
3	2627.8	(5793.2)	2933.7	(6467.8)	3794.5	(8365.5)
4	2577.7	(5682.8)	2790.4	(6151.7)	3238.8	(7140.4)
5	2524.6	(5565.8)	2701.5	(5955.8)	2992.0	(6596.2)
6	2466.7	(5438.2)	2632.6	(5803.9)	2877.1	(6343.0)
7	2401.4	(5294.2)	2570.5	(5666.9)	2790.2	(6151.3)
8	2358.8	(5200.3)	2509.2	(5531.8)	2720.4	(5997.5)
9	2318.6	(5111.6)	2445.3	(5390.9)	2660.4	(5865.2)
10	2301.9	(5074.8)	2378.4	(5234.5)	2605.2	(5743.4)
11	2297.6	(5065.4)	2336.8	(5151.8)	2552.1	(5626.3)
12	2295.8	(5061.3)	2318.7	(5111.8)	2499.8	(5511.0)
13	2295.6	(5060.9)	2309.4	(5091.4)	2449.9	(5401.0)
14			2304.2	(5079.8)	2404.8	(5301.6)
15			2302.8	(5076.8)	2368.8	(5222.3)
16			2302.8	(5076.7)	2348.3	(5177.0)
17					2331.6	(5140.3)
18					2319.8	(5114.2)
19					2311.1	(5095.1)
20					2304.9	(5081.4)

at all) and the need for a significant increase in cycles as the move limits decrease. This table also illustrates that, with the largest move limit, the ACCESS 3 program matches the minimum feasible weight and number of design cycles that have been reported to date.

Adverse effects of the small move limits can be attributed to the following:

1) Restricting the rate of design variable changes also restricts the rate of design improvement.

2) A destabilizing effect in the Lagrange multiplier computations can occur when the composition of the sets of active and passive design variables oscillates or changes rapidly. The consequences are that the Jacobian matrix [Eq. (14)] changes accordingly and the search direction is valid only for short distances along the search line [Eq. (12)].

3) There can be so many side-bounded design variables that there are fewer free design variables than active-constraint equations. This situation will cause the Jacobian matrix to be singular.

In the attempt to remedy side boundary problems, several optional strategies have been implemented and tested with at least partial success. These are:

1) *Relaxation of lower bounds for secondary members.* Members of customary structures can frequently be categorized as primary, for which large sizes are favorable, or as secondary and nearly redundant, for which the sizes should be as small as possible. Members that meet either of the following two conditions could reasonably be categorized as secondary: a) the right-hand side of Eq. (7) is negative, and b) the size of the member as determined by the optimality criterion is less than the move limit bound and less than the stress ratio bound. Then, for members in these categories, the lower bound a is replaced by a' (Fig. 4).

2) *Side bound stabilization.* This option applies only during the solution for the Lagrange multipliers and is an attempt to stabilize the computations by ignoring the side bounds whenever the right-hand side of Eq. (7) is positive. After completion of the solution for the multipliers of the current set of active-constraint equations, the design variables are checked for side bound violations before the next active constraint to be added is selected, and are adjusted as necessary.

3) *Adjusted move limit computations.* When this strategy is applied, move limits are computed [Eq. (22)] for a

hypothetical current design that has been uniformly scaled to feasible. Invoking this option makes the design independent of proportional change of the chosen starting value. Adjusted scaling can have a favorable result when the start design is predominantly oversized and exceeds feasibility. However, there can be an unfavorable result for an undersized starting design because the lower bounds for secondary members become too high. Move limit adjustment has been found to provide a significant advantage when a few initial cycles of fully stressed design are used as a prelude to optimization formulation. When optimization is used in the first cycle, this option is not always advantageous.

Demonstration Problems

Many of the strategy options described have been included in a set of design executions that match the move limit conditions of Table 1. Table 2 shows the corresponding design histories obtained with our current research computer program. The strategy options used for the designs were identical and are listed below:

1) When attempts to obtain a starting value for the first multiplier of the active set [Eq. (19)] failed because all side bounds became active, the starting value reverted to that found at the first attempt.

2) Decoupled estimates for the starting values of multipliers added to the active set were made through the fourth cycle. After that, the value existing from a prior cycle was used except for the first multiplier in the set.

3) Relaxation of lower side bounds for secondary members was permitted. During execution, the option was occasionally invoked for the problems with the lower move limit during the first few cycles.

4) Side bound stabilization was used during Newton method solutions.

5) Move limit computations did not use feasibility scaling.

A comparison of Table 2 with Table 1 shows that the feasible weights attained are all within 0.2 kg (0.5 lbm) of the known minimum and that the difficulties in obtaining convergence for move limits of 1.40 and 1.75 have been predominantly overcome. A surprising result that appears in Table 2 is the convergence to almost the minimum weight for both $R = 1.75$ and $R = 1.40$ in only 11 cycles, which seems to be 2 cycles less than reported for any previous execution of this problem.

Table 2 Research program histories for 10-bar truss

Cycle	Structure mass scaled to feasible, kg (lbm)					
	$R = 50.00$		$R = 1.75$		$R = 1.40$	
1	3749.4	(8266.1)	3749.4	(8266.1)	3749.4	(8266.1)
2	2728.9	(6016.2)	2923.7	(6445.6)	3057.1	(6739.8)
3	2637.0	(5813.6)	2656.2	(5856.0)	2750.3	(6063.3)
4	2607.9	(5749.4)	2584.1	(5696.9)	2581.3	(5690.8)
5	2556.9	(5636.4)	2557.0	(5637.2)	2553.4	(5629.3)
6	2501.3	(5514.4)	2501.7	(5515.2)	2497.8	(5506.6)
7	2439.8	(5378.8)	2440.2	(5379.7)	2439.3	(5377.8)
8	2366.9	(5218.1)	2380.0	(5247.1)	2407.8	(5308.2)
9	2314.5	(5102.7)	2301.2	(5073.2)	2305.7	(5083.3)
10	2302.0	(5075.1)	2296.3	(5062.4)	2298.9	(5068.2)
11	2297.9	(5066.0)	2295.6	(5060.9)	2295.7	(5061.1)
12	2296.3	(5062.4)				
13	2295.6	(5060.9)				

Table 3 Summaries of fully stressed designs, 10-bar truss, move limit = 1.40

	Number of fully stressed design cycles			
	0	1	2	3
Number of optimization cycles	13	11	9	8
Total number of cycles	13	12	11	11
Mass, kg (lbm)	2295.6 (5060.9)	2295.6 (5060.9)	2295.6 (5060.9)	2295.6 (5060.9)

Table 4 63-bar space truss design histories

Cycle	Feasible weight, kg (lbm)							
	ACCESS 3				Research program			
	Standard		Partial FSD		No primary stress constraints		13 primary stress constraints	
1	13705	(30,214)						
2	3435	(7573)	3459	(7625)	2885	(6360)	3323	(7326)
3	2969	(6546)	3192	(7037)	2705	(5963)	2922	(6441)
4	3054	(6733)	3121	(6880)	3607	(7953)	3541	(7807)
5	2854	(6292)	2953	(6510)	2883	(6355)	2879	(6347)
6	2832	(6243)	2898	(6388)	2896	(6385)	2877	(6343)
7	2813	(6201)	2851	(6286)	2846	(6274)	2822	(6222)
8	2795	(6161)	2820	(6216)	2831	(6241)	2809	(6193)
9	2781	(6132)	2801	(6175)	2818	(6213)	2806	(6186)
10	2777	(6123)	2789	(6149)	2809	(6192)	2788	(6146)
11	2776	(6121)	2784	(6137)	2803	(6179)		
12	2776	(6120)	2781	(6130)				
13	2776	(6119)						
Relative net computation time	1.00		0.38		0.05		0.14	

An attempt to explore execution time reduction was made by replacing the optimization design method with the fully stressed design method for several of the initial design cycles. During these cycles, all primary stress and displacement constraints were removed and members had stress ratio side constraints.

Table 3 contains a summary of the feasible weights achieved for several variations in the number of initial fully stressed design cycles. The first column of results is for no initial fully stressed design cycles and shows two more design cycles than Table 2. These extra cycles occur because the move limit scaling adjustment option, which was found to be advantageous starting from a fully stressed design, was used. The option was invoked for the first six (independent of design mode) cycles in all cases. The first column is a rerun of the earlier execution made to provide a more equitable comparison. All other options used previously were maintained. In examining this table, it is valid to assume a saving (because of the relative computational simplicity in computer time) whenever the total number of cycles with fully stressed design is no more than with none.

63-Bar Space Truss Example

This simple test problem is a simulation of an aircraft wing structural component. Figure 6 is a schematic outline of the structure. (Full details of the model and optimization problem specification can be found in Ref. 8.) The loading is applied to the two nodes at the tip, as indicated in the figure, and consists of two combinations of forces that apply torsion to the structure. The maximum relative lateral displacement of the two tip nodes for either of the two loadings is specified.

Representing all stress constraints as primary, feasible weights of about 2776 kg (6120 lbm) have been achieved in from 10 to 13 cycles.^{1,12} When only the two displacement constraints were used as primary and the remainder treated by stress ratio, a weight about 0.5% larger was obtained,⁸ but with many more design cycles.

In the present work, the first formulation of the problem was to retain only the displacement constraints as primary, and use the stress ratios to design for all of the member stresses. The second formulation of the problem added 13 primary constraints for the stresses of selected members. The selection was made by examining results of the first formulation and by attempting to identify the members that were most frequently responsible for overstresses during the several design cycles.

The design histories are shown in Table 4. The "standard" results tabulated here for ACCESS 3 represent the usual mode

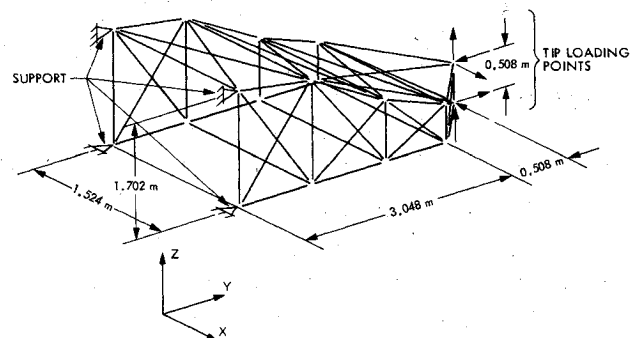


Fig. 6 63-bar space truss schematic.

of operation, in which most of the stress constraints are allowed to qualify as primary constraints. The "partial FSD" column represents relaxation of an acceptance criterion to permit a larger number of stress constraints to be treated by the stress ratio method rather than by primary constraints.

The ACCESS 3 results are reproduced from Ref. 12; the same problems were also performed with this program on our computer. Because of our own executions with ACCESS 3 and information developed for separating the central processor unit (CPU) time for computations from the CPU time for printing, we are able to estimate the net times for computation in absence of all printing. These estimates are the basis of the relative computation times shown in the last row of the table.

It can be seen that our current research program produces a weight that is from 0.5 to 1.0% heavier than the smallest weight shown, although with substantially less computation time. Nevertheless, it is only fair to acknowledge that the results presented are the most favorable we obtained from a number of trials with changes in option parameters. Parameters different from those added for the tabulated executions occasionally added as much as 45 kg (100 lbm).

The table also makes it evident for both the ACCESS 3 program and the research program that, employing primary stress constraints rather than stress ratio side constraints can provide moderate reductions in final weight at the expense of significant increases in computation time.

Summary and Conclusions

The Lagrange multiplier method, although possibly the simplest conceptually, appears to be the most powerful and practical for application to design problems with medium to

large structures. The outstanding attribute of the method is the reduction of the design space from design variable size to active-constraint size. A primary difficulty of the method, which has historically been considered formidable, is the need to identify the subset of active constraints for which multipliers must be determined. This difficulty, however, appears predominantly to have been overcome by the strategy developed elsewhere by Schmit and Fleury.³ Beyond this, however, additional strategies that relate to implementation of the method and that are capable of dealing correctly with many problem-dependent or user-initiated opportunities for pathological behavior require effective development.

Strategies proposed and tested here have been useful on some of the examples considered and often have matched or possibly exceeded the best solutions obtained otherwise. Nevertheless, solution of the last example problem treated is considered to have been only partly successful in that a lower structure weight attained elsewhere was exceeded. However, the small percentage of excess weight may be significant only in a mathematical rather than a practical sense. One reason for the higher weight was the attempt to employ side constraint stress ratio bounds to replace primary stress constraints. This restriction of the number of primary constraints appears to be essential to limit the amount of computation time when processing production problems that are substantially larger than most conventional problems.

In problems much larger than these, the time required to apply the design optimization algorithms depend only upon the number of design variables. Consequently, the increased time for this phase may not be significant if comparable numbers of design variables are present. However, on the other hand, each potentially active stress constraint requires a load-deflection analysis or at least the equivalent to determine a virtual work or similar parameter for that constraint. These extra load-deflection analyses could be extremely time-consuming and dominate the time for stiffness matrix decomposition, which usually predominates in the time for static structure analysis. It is evident that there is a need for better strategies to economize the number of primary constraints to be called upon in the design problem solution.

Acknowledgment

The research described in this publication was carried out by the Jet Propulsion Laboratory, California Institute of Technology, under NASA Contract NAS7-100.

References

- ¹Schmit, L. and Mura, H., "Approximation Concepts for Efficient Structural Synthesis," NASA CR-2552, March 1976.
- ²Khot, N., Berke, L., and Venkayya, V., "Comparison of Optimality Criteria Algorithms for Minimum Weight Design of Structures," *AIAA Journal*, Vol. 17, Feb. 1979, pp. 182-190.
- ³Schmit, L. and Fleury, C., "An Improved Analysis/Synthesis Capability Based on Dual Methods—Access 3," *Proceedings of the AIAA/ASME/SAE 20th Structures, Structural Dynamics and Materials Conference*, April 1979.
- ⁴Fleury, C., "An Efficient Optimality Criteria Approach to the Minimum Weight Design of Elastic Structures," *Computers and Structures*, Vol. 11, 1980, pp. 163-173.
- ⁵Levy, R. and Chai, K., "Implementation of Natural Frequency Analysis and Optimality Criterion Design," *Computers and Structures*, Vol. 10, 1979, pp. 277-282.
- ⁶Luenberger, D. G., *Introduction to Linear and Nonlinear Programming*, Addison-Wesley, Reading, Mass., 1973, Chap. 10.
- ⁷Levy, R., "Computer-Aided Design of Antenna Structures and Components," *Computers and Structures*, Vol. 6, 1976, pp. 419-428.
- ⁸Berke, L. and Khot, N., "Use of Optimality Criteria Methods for Large Scale Systems," *On Structural Optimization*, AGARD Lecture Series No. 70, Oct. 1974, pp. 1-29.
- ⁹Melosh, R. and Luik, R., "Approximate Multiple Configuration Analysis and Allocation for Least Weight Structural Design," AFFDL-TR-67-59, April 1967.
- ¹⁰Segenreich, S., Zouain, N., and Herskovits, J., "An Optimality Criteria Method Based on Slack Variables Concept for Large Scale Structural Optimization," *Symposium on Applications of Computer Methods in Engineering*, School of Engineering, University of Southern California, Los Angeles, Aug. 1977, pp. 563-572.
- ¹¹Levy, R. and Melosh, R. J., "Computer Design of Antenna Reflectors," *Journal of the Structural Division, Proceedings of the ASCE* 99 (ST-11), Paper 10178, Nov. 1973, pp. 2269-2285.
- ¹²Fleury, C. and Schmit, L., "Dual Methods and Approximation Concepts for Structural Synthesis," NASA CR 3226.

37- 36- 35- 34- 33- 32- 31- 30- 29- 28- 27- 26- 25- 24- 23- 22- 21- 20- 19- 18- 17- 16- 15- 14- 13- 12- 11- 10- 9- 8- 7- 6- 5- 4- 3- 2- 1-